THE JOURNAL OF BIOLOGICAL CHEMISTRY
Vol. 276, No. 36, Issue of September 7, pp. 33681–33688, 2001

Printed in U.S.A.

Electron Spin Resonance and Fluorescence Studies of the Bound-state Conformation of a Model Protein Substrate to the Chaperone SecB*

Received for publication, May 16, 2001, and in revised form, June 26, 2001
Published, JBC Papers in Press, July 2, 2001, DOI 10.1074/jbc.M104466200

Vikram G. Panse‡§, K. Beena‡, Reinhard Philipp¶, Wolfgang E. Trommer¶, Pia D. Vogel¶, and Raghavan Varadarajan‡‖****

From the ‡Molecular Biophysics Unit, Indian Institute of Science, Bangalore 560 012, India, ‖Chemical Biology Unit, Jawaharlal Center for Advanced Scientific Research, Jakkur P. O., Bangalore 560 004, India, and ¶Fachbereich Chemie/Abteilung Biochemie der Universitat Kaiserslautern, Erwin Schrodinger Str., 67663 Kaiserslautern, Germany

SecB is a homotetrameric, cytosolic chaperone that forms part of the protein translocation machinery in *Escherichia coli*. We have investigated the bound-state conformation of a model protein substrate of SecB, bovine pancreatic trypsin inhibitor (BPTI) as well as the conformation of SecB itself by using proximity relationships based on site-directed spin-labeling and pyrene fluorescence methods. BPTI is a 58-residue protein and contains three disulfide groups between residues 5 and 55, 14 and 38, as well as 30 and 51. Mutants of BPTI that contained only a single disulfide were reduced, and the free cysteines were labeled with either thiol-specific spin labels or pyrene maleimide. The relative proximity of the labeled residues was studied using either electron spin resonance spectroscopy or fluorescence spectroscopy. The data suggest that SecB binds a collapsed coil of reduced unfolded BPTI, which then undergoes a structural rearrangement to a more extended state upon binding to SecB. Binding occurs at multiple sites on the substrate, and the binding site on each SecB monomer accommodates less than 21 substrate residues. In addition, we have labeled four solvent-accessible cysteine residues in the SecB tetramer and have investigated their relative spatial arrangement in the presence and absence of the substrate protein. The electron spin resonance data suggest that these cysteine residues are in close proximity (15 Å) when no substrate protein is bound but move away to a distance of greater than 20 Å when SecB binds substrate. This is the first direct evidence of a conformational change in SecB upon binding of a substrate protein.

Molecular chaperones are a class of proteins that prevent aggregation of newly synthesized or previously denatured polypeptides and proteins and mediate their folding into the native state (1). The common property shared by most molecular chaperones is the ability to recognize structural elements exposed in unfolded or partially denatured states such as hydrophobic surfaces. They do not bind the native state of proteins and are capable of interacting with a variety of different polypeptide chains, often without apparent sequence preferences (1, 2). SecB is a tetrameric chaperone in *Escherichia coli* that is involved in the translocation of polypeptide chains into the periplasmic space of the cell (3). *In vivo*, SecB binds to a subset of precursor proteins and maintains them in an unfolded, translocation-competent state, whereas *in vitro* it interacts with a variety of proteins in the non-native state (4–7). The nature of the translocation-competent state of substrate proteins is unknown, although it is believed to be a flexible molten globule state (8). For some proteins the translocation-competent state contains significant secondary and tertiary structure (4). Studies on the model protein substrate, barstar, revealed that SecB does not bind the folded or unfolded state but traps a near native-like molten globule state (6). SecB has also been shown to bind partially folded states of lactalbumin (9).

Bovine pancreatic trypsin inhibitor, BPTI,[1] has been extensively used as a model protein for folding studies. It consists of 58 residues and is stabilized by three disulfide bonds between the amino acids 5 and 55, 14 and 38, as well as 30 and 51. The stability of BPTI is directly linked to the formation of these three disulfide bonds, and reduction of the disulfides results in unfolding of the protein. Both non-native and native disulfide intermediates formed during the folding of BPTI have been well characterized (10–12). The structures of single disulfide intermediates and of unfolded BPTI have also been characterized (10–13). Various biophysical measurements suggest that reduced BPTI can exist in a compact conformation that is almost devoid of secondary structure elements (14- 20). BPTI is a convenient model substrate to study interactions between SecB and substrate proteins. The kinetics and thermodynamics of the interaction of SecB with reduced, unfolded BPTI has previously been characterized (10). It was shown that SecB binds to reduced, unfolded BPTI with a stoichiometry of one BPTI molecule per SecB monomer, a K_d in the nanomolar range, and an on-rate that is close to diffusion controlled rates.

* This work was supported by grants from Department of Science and Technology and Department of Biotechnology (to R. V.), by Bundesministerium für Bildung und Forschung Grant INI-257-95, and by Fonds der Chemischen Industrie (to W. E. T.). The costs of publication of this article were defrayed in part by the payment of page charges. This article must therefore be hereby marked "*advertisement*" in accordance with 18 U.S.C. Section 1734 solely to indicate this fact.

§ Recipient of a Journal of Cell Science Fellowship from the Company of Biologists, United Kingdom and the Wood-Whelan Research Fellowship, International Union of Biochemistry and Molecular Biology.

** Recipient of the Swarnajayanthi Fellowship, Government of India and a Senior Research Fellow of the Wellcome Trust. To whom correspondence should be addressed. Fax: 91-80-3600535 or 3600683; E-mail: varadar@mbu.iisc.ernet.in.

[1] The abbreviations used are: BPTI, bovine pancreatic trypsin inhibitor; (*X*-*Y*), BPTI that has free thiols at positions *X* and *Y*, where *X* and *Y* are 5–55 or 14–38 or 30–51; $(X\text{-}Y)_{Py}$, BPTI labeled at positions *X* and *Y* with pyrene maleimide; $(X\text{-}Y)_{SL}$, BPTI labeled at positions *X* and *Y* with a spin label (SL); $(BPTI)_{all\ Ala}$, completely unfolded BPTI, with alanine residues substituted for all normally occurring cysteines; IOPI, 4-(3-iodo-2-oxypropylidene-1-)-2,2,3,5,5-pentamethyl-imidazolidine-1-oxyl; ESR, electron spin resonance; MALDI, matrix-assisted laser desorption ionization; MS, mass spectroscopy.

ESR spectroscopy using site-specific spin labeling of unique cysteine residues has been used successfully in recent years to study protein structures and structural changes in a variety of different proteins and enzymes (21). The approach has been further extended to measure distances between two site-specifically placed spin-labels by calibrating spectral components to the distances derived from well known helical structures of peptides (22). A similar approach has been employed recently to determine the proximity of helices and their relative movement upon photoactivation in bacteriorhodopsin (23, 24).

A second biophysical technique that has been used to study proximity of residues in proteins is pyrene excimer fluorescence (25). Pyrene excimer fluorescence has been extensively used to determine proximity of residues in helices of the membrane protein lac permease (26, 27). Determination of inter-residue distances provides a strategy to deduce the proximity of selected secondary structural elements and therefore allows insight into the global structure or structural changes of a protein at the level of the backbone fold (21). In the present work, we have used unfolded BPTI as a model substrate to gain insights into the bound state conformation of polypeptides interacting with the chaperone SecB. We have investigated the binding of SecB to several BPTI mutants that were labeled at two Cys residues with either pyrenes or spin labels. Single disulfide mutants of BPTI in which alanines had been substituted for the other cysteine residues were used. The mutant proteins were labeled in the reduced state with either the spin labels or pyrene maleimides, and the proximity of the labeled residues was studied using fluorescence methods and ESR spectroscopy.

MATERIALS AND METHODS

Protein Purification—The SecB expression plasmid pJW25 in strain BL21 (DE3) was obtained from B. de Kruijff, Utrecht University. SecB purification was done as reported previously (6). The purified protein was estimated to be 99% pure by SDS-polyacrylamide gel electrophoresis as detected by silver staining (28) and analytical gel filtration high performance liquid chromatography. The extinction coefficient at 280 nm was taken to be 11,900 M^{-1} cm^{-1} for monomeric SecB (29). All the SecB concentrations reported here refer to monomers of SecB unless otherwise stated. Purification of the single disulfide BPTI mutants was performed as described (10, 12, 20, 30).

Pyrene- and Spin-labeling of SecB and BPTI—4-(3-Iodo-2-oxypropylidene-1-)-2,2,3,5,5-pentamethyl-imidazolidine-1-oxyl (IOPI) was prepared as described in Volodarsky (31).1 mg of the single disulfide mutants of BPTI were reduced in 200 μl of 6 M guanidine hydrochloride in Tris-HCl, pH 8.8, containing 10 mM dithiothreitol. The reaction mixture was desalted on a PD-10 column (Amersham Pharmacia Biotech) and lyophilized. The reduced proteins were dissolved in 200 μl of 6 M guanidine hydrochloride in potassium phosphate buffer, pH 7.4, and 50 μl of a 20 mM solution of IOPI in *N*,*N*-dimethylformamide was added. The mixture was then incubated for 1 h in the dark at 25 °C, desalted on a PD-10 column, and lyophilized. For pyrene labeling, reduced protein was dissolved in 200 μl of 6 M guanidine hydrochloride in potassium phosphate buffer, pH 7.4, as described above, and 50 μl of a 20 mM solution of pyrene maleimide in *N*,*N*-dimethylformamide was added. The reaction mixture was again incubated for 1 h in the dark at room temperature, desalted on a PD-10 column, and lyophilized. The extent of labeling was assayed according to Creighton (32) and found to be 1.9 Cys residues/BPTI molecule. To label SecB with pyrene maleimide or IOPI-spin label, a similar procedure was carried out as described above except that guanidine hydrochloride was excluded from the reaction mixture to avoid denaturation of the protein.

The oligomeric state of the protein after cysteine modification was analyzed by subjecting both labeled and unlabeled SecB to gel filtration on a Superdex 75 HR 10/30 (Amersham Pharmacia Biotech) gel filtration column. The column was equilibrated with 50 mM sodium phosphate buffer, pH 7.4, containing 150 mM NaCl.

The extent of spin- or pyrene-labeling was assayed by determining the amount of residual, unreacted SH groups as described previously. Both under denaturing and under non-denaturing conditions, three unreacted sulfhydryl groups were found per monomer, suggesting that only one of the four cysteines per monomer was modified by our reagents. Similar results were described earlier (33).

In the case of the pyrene-labeled SecB, the extent of labeling was also analyzed by mass analysis. Positive ESI-MS of the unlabeled and the pyrene-labeled SecB was recorded on a Hewlett Packard Series 1100 mass selective detector mass spectrometer to confirm the presence of a single pyrene chromophore per SecB monomer. Detection of the uniquely labeled cysteine was done by carrying out CNBr cleavage on the tryptic digest of the unlabeled and the pyrene-labeled SecB as described (34). MALDI of the peptide mixtures was performed on a Kompact SEQ mass spectrometer (Kratos Analytical). 10 mg/ml α-cyano-4-hydroxy-cinnamic acid in acetonitrile/methanol/water, 5:3:2, was used as a matrix solution, and the spectra were obtained in the linear mode.

ESR Measurements—The ESR measurements were carried out using a Bruker ESP 300 E spectrometer operating in the X-band mode. A dielectric cavity TE_{011} (ER 4118) was used for all experiments. 20-μl aliquots of the spin-labeled proteins in 100 mM potassium phosphate buffer, pH 7.4, were prepared in sealed quartz capillaries. Spectra of the samples at room temperature (298 K) were obtained by averaging 3–5 scans at a scan width of 120 Gauss. The microwave power was set to be 2 mW, and the modulation amplitude was optimized to the line-width of the individual spectra. ESR spectra in the frozen state (183 K) were recorded at a microwave power of 0.05 mW.

Fluorescence Measurements—All fluorescence emission experiments were carried out using a Jasco FP 777 fluorimeter. The fluorescence measurements were carried out in a 1-cm quartz cuvette at 25 °C with an excitation wavelength of 344 nm. To obtain the excitation spectra, the excitation wavelength was varied from 320 to 360 nm, and the fluorescence was monitored at 377 nm and 450 nm for monomer and excimer fluorescence, respectively. A slit width of 1.5 nm was used for measuring both excitation and emission. The binding affinity of the different pyrene-labeled BPTI mutants for SecB was carried out as follows. 25 nM labeled BPTI in 100 mM potassium phosphate buffer was taken in the cuvette held at 25 °C. Increasing amounts of SecB from 10 to 500 nM were added, and the increase in fluorescence intensity at 400 nm was recorded. The data were analyzed as described (5, 9) to obtain the dissociation constant.

Homology Modeling of E. coli SecB Structure—Comparative protein structure modeling program MODELLER (35) was used for the model building of the *E. coli* SecB structure. The program was downloaded from the MODELLER homepage on the Internet. Multiple sequence alignment of eight bacterial SecB proteins using ClustalW shows that the *E. coli* SecB has 60% sequence identity with the *Hemophilus influenzae* SecB. Three of the four cysteines, corresponding to the positions 76, 97, and 102, are conserved, whereas leucine is present at the position of the *H. influenzae* SecB that corresponds to Cys-113 of the *E. coli* SecB. The crystal structure of the *H. influenzae* SecB (36) was then used as the template structure.

The crystal structure reveals that SecB is organized as a dimer of dimers. The solvent accessibility of the cysteine residues was determined using the programs DEPTH (37) and ACCESS (38) and the coordinates of the crystal structure of SecB. The results from these two programs indicated that the cysteines in each monomer are accessible to slightly different extents. Hence, we modeled the *E. coli* SecB for the four monomers independently, taking the monomers of the *H. influenzae* SecB as templates. The four modeled monomers were combined to give the modeled structure of the tetrameric protein. The accessibility of the cysteines was then determined by using the programs DEPTH and ACCESS on the modeled structure. The distances between the Sγ of the cysteines was determined using RASMOL. A bound IOPI spin-label at position 97 was also modeled on the modeled structure of *E. coli* SecB tetramer using the programs Quanta 97 and CharmM 2.3 (Molecular Simulations) for modeling and energy minimization. The nitroxide group of the IOPI spin-label is at a distance of about 7.5 Å from the position of the corresponding cysteine residue. The modeling was done to determine the distance between the nitroxide radicals in the IOPI-labeled cysteines.

RESULTS

Reduced, unfolded BPTI has been previously shown to bind to SecB (5, 7). However, little is known about the regions of the substrate that are involved in binding, the conformation of bound substrate, and whether substrate binding is accompanied by a change in SecB conformation. We have used two different approaches to obtain this information. In a first set of experiments, we have incorporated into unfolded BPTI a pair of

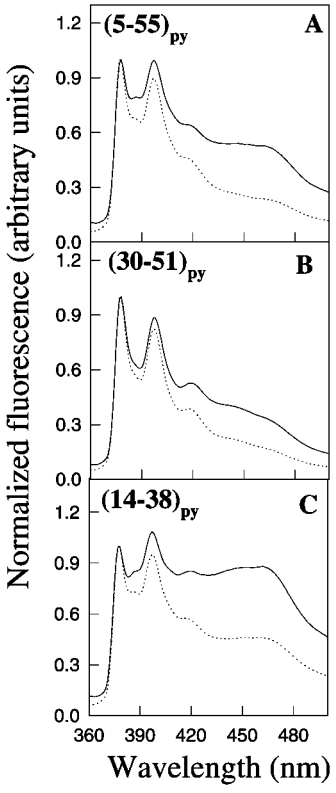

FIG. 1. **Normalized fluorescence spectra of pyrene-labeled BPTI mutants at 25 °C, pH 7.4.** The fluorescence spectra were normalized to have an identical intensity at 377 nm. *A*, 1 μM $(5–55)_{Py}$ alone (*solid line*) and in complex with 10 μM SecB (*dotted line*). *B*, 1 μM $(30–51)_{Py}$ alone (*solid line*) and in complex with 10 μM SecB(*dotted line*). *C*, 1 μM $(14–38)_{Py}$ alone (*solid line*) and in complex with 10 μM SecB (*dotted line*).

either spin labels or fluorescent labels at various positions along the primary sequence to investigate the proximity of the labels relative to each other in the free as well as the SecB-bound state. In a second approach, the four solvent-accessible cysteine residues on SecB were labeled to study potential structural changes of the chaperone upon binding the permanently denatured $(BPTI)_{all\ Ala}$.

Pyrene Fluorescence of BPTI Mutants—The single disulfide mutants of BPTI 5–55, 30–51, and 14–38 were labeled with pyrene maleimide, and the labeling efficiency was checked as described under "Materials and Methods." The fluorescence emission spectrum of pyrene (excited at 345 nm) is composed of two bands, a structured band with peaks near 385 and 405 nm, which is referred to as the monomer peak, and an unstructured broad peak near 470 nm that is observed when two pyrenyl groups are close to each other at a distance of ~3.5 Å (excimer band). Upon binding of the labeled mutants of BPTI to SecB, an increase in fluorescence intensity is observed, indicating that the pyrene probes are in a hydrophobic environment upon binding to the chaperone as described previously (39). Fig. 1 shows the pyrene emission of labeled BPTI mutants in the presence (*dotted lines*) and absence (*solid lines*) of SecB. The addition of SecB to labeled BPTI results in changes in fluorescence intensities of both monomer and excimer peaks. These changes are due in part to decreased quenching of pyrene fluorescence by solvent in the SecB-bound state. Hence, to analyze intensities of the excimer peak in the presence of SecB, the spectra were normalized to have identical intensity at 377 nm both in the presence and absence of SecB. Pyrene modifications at the amino acid positions 5 and 55 or 30 and 51 (Fig. 1, *A* and *B*, *solid lines*) show relatively weak excimer fluorescence, indicating that in both sets of mutants, the chromophores are at distances greater than 3.5 Å. Stronger excimer fluorescence is observed when the labels were in positions 14 and 38 (Fig. 1, *C*, *solid line*). Upon binding of the labeled BPTI to SecB, the weak excimer fluorescence of the mutants with the labeled residues $(5–55)_{Py}$ and $(30–51)_{Py}$ decreased even further (Fig. 1, *A* and *B*, *dotted lines*). Also in the case of labeled residues $(14–38)_{Py}$ (Fig. 1*C*, *dotted line*), a large decrease in excimer fluorescence is observed upon the addition of SecB, although some excimer fluorescence remained.

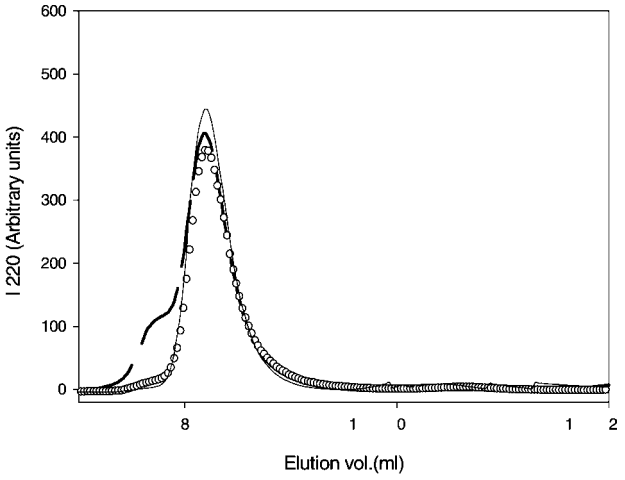

FIG. 2. **Size exclusion chromatography of SecB.** Unlabeled and labeled SecB were subjected to fast protein liquid chromatography on a Superdex 75 HR 10/30 gel filtration column as described under "Materials and Methods." The *dashed line*, *open circles*, and *solid line* represent pyrene-labeled SecB, spin-labeled SecB, and unlabeled SecB, respectively. The shoulder, present for pyrene-labeled protein at the void volume of the column, probably results from the presence of some aggregated species.

Determination of the Site of Attachment of the Thiol Label to Native SecB—We have labeled the four solvent-accessible cysteine residues in SecB (one Cys per monomer) using pyrene maleimide (33). Modification of the cysteine residue in SecB by 5,5′-dithiobis(nitrobenzoic acid) is reported to cause irreversible dissociation of the tetramer to dimer (40). Hence, both pyrene-labeled and the unlabeled SecB were analyzed by gel chromatography to check for the oligomeric state of the protein after labeling. Pyrene-labeled SecB elutes at the same position as the unlabeled SecB. This indicates that both labeled and unlabeled proteins exist primarily as tetrameric species in solution and that no dimer is present (Fig. 2). The shoulder in the gel filtration profile of the pyrene-labeled SecB, appearing in the void volume of the column, could be indicative of the presence of a small fraction of aggregate. However no aggregated species is present for the spin-labeled protein.

5,5′-Dithiobis(nitrobenzoic acid) labeling as well as the ESI-MS of the pyrene-labeled SecB confirmed pyrene labeling of a single cysteine per SecB monomer (Fig. 3*A*). Although there are four cysteines in SecB monomer at the positions 76, 97, 102, and 113 that can be selectively modified by thiol-labeling reagents, MALDI of the proteolysed mixture of the pyrene-labeled SecB showed that only the peptide fragment 95–111 contains a cysteine with a single pyrene (Fig. 3, *B* and *C*). Thus either cysteine 97 or cysteine 102 is likely to be the site of labeling. Since the two cysteines are very close to each other in the primary sequence, it was not possible to experimentally determine which of the two was the actual site of labeling using this technique. We therefore modeled the *E. coli* SecB as described under "Materials and Methods." Table I summarizes the relative accessibility in both the crystal struc-

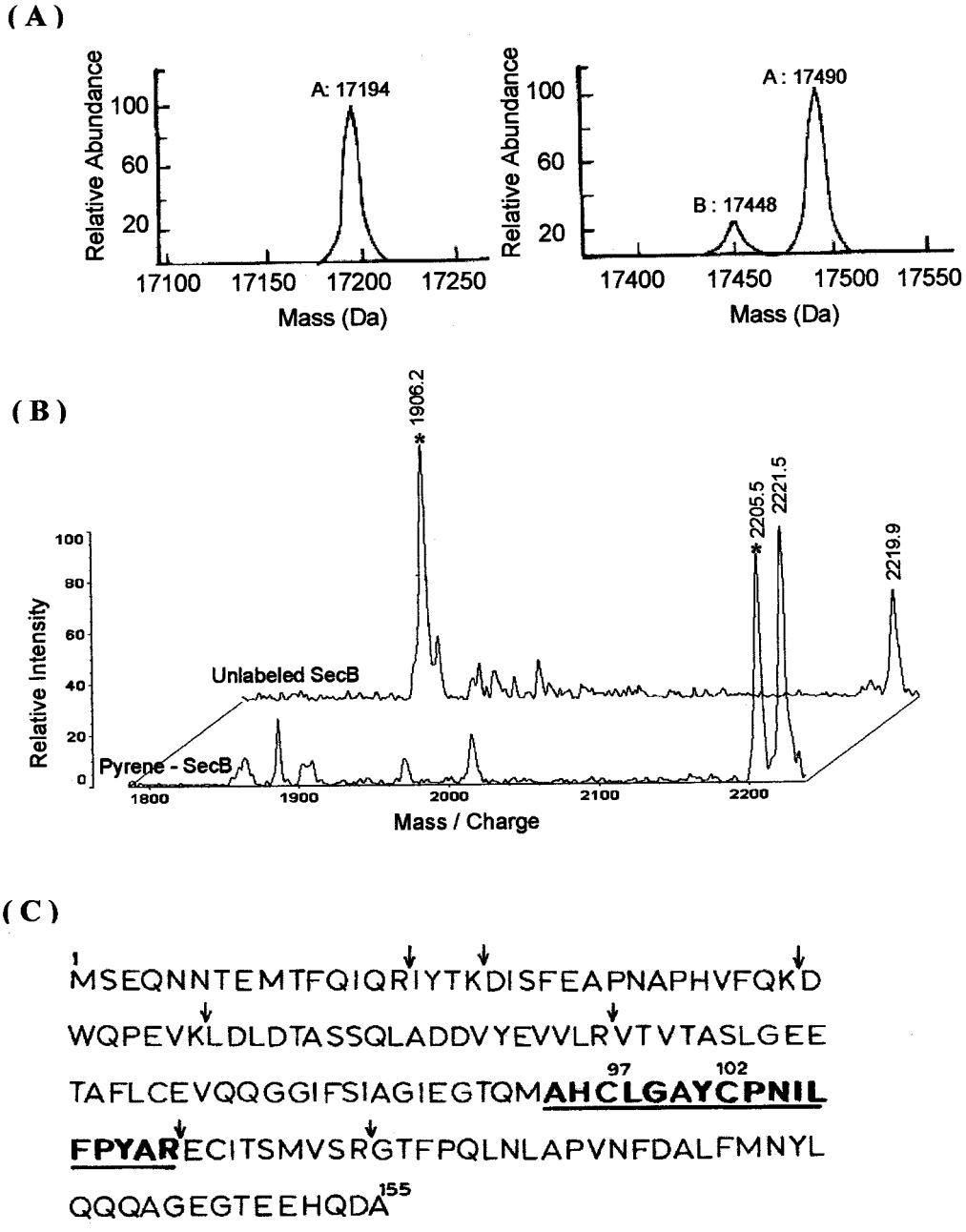

FIG. 3. *A*, ESI-MS of the SecB monomer. Positive ion mass spectrum of SecB in acetonitrile, pH 3.0. In *panel I*, peak *A* denotes the acetylated form of SecB (17,189 + 5D). In *panel II*, peak *A* and peak *B* denote the single pyrene-labeled acetylated (17,486 + 4D) and nonacetylated (17,442 + 6D) form of SecB respectively. *B*, MALDI-time of flight mass spectra of SecB after Trypsin/CNBr treatment. The *asterisks* indicate the peak corresponding to the peptide fragment 95–111. The front and back spectra are for the pyrene-labeled and the unlabeled SecB, respectively. *C*, peptide fragments from trypsin digestion of SecB. The *arrows* indicate the trypsin cleavage sites. The single cysteine that can be covalently labeled in native SecB lies within the stretch of residues from 95–111 that is *underlined* and in *bold*. This was determined by subjecting the tryptic digest of the labeled protein to CNBr cleavage and the analysis by MALDI-time of flight as described in *panel B* above.

ture and the modeled structure. The table shows that with the exception of chain A, residue 97 is the most accessible in both the crystal and model structures. For chain A, Cys-102 is most exposed in the model, and Leu-122 (equivalent to Cys-113 in *E. coli* SecB) is most exposed in the crystal structure. It is possible that Cys-97 is labeled in three chains, and in chain A either no Cys is labeled or either Cys-102 or Cys-113 is labeled. Previous 5,5′-dithiobis(nitrobenzoic acid) labeling studies showed that four Cys residues are labeled per tetramer (33). Mass spectrometric studies did not show any evidence for labeling of Cys-113. Taken together the data suggest that either Cys-97 is labeled in all chains or that Cys-102 is labeled in chain A, and Cys-97 is labeled in the remaining chains. The pyrene-labeled SecB was further characterized by fluorescence spectroscopy. No excimer formation was observed (data not shown). This indicates that the pyrenes are held rigidly at a distance of more than 3.5 Å and are probably part of a secondary structural element of the protein. The inter-cysteine distances for the two cysteine residues, 97 and 102, that are the most probable sites of labeling, are indeed greater than 3.5 Å in the structure (Table IB). The addition of the unfolded $(BPTI)_{all\ Ala}$ mutant leads to an increase in fluorescence of the labeled pyrenes of SecB, indicating a change in the environment upon binding of the substrate molecules. This is suggestive of a conformational transition of the chaperone upon binding of the substrate protein. Alternatively the substrate binding may occur close to the site of the pyrene label on SecB. ESR studies described below, however, support the first possibility.

TABLE I

A. Accessibility (%) of the cysteine residues in the modeled E. coli SecB and in the crystal structure of H. influenzae *SecB. Homologous positions in the two structures are in the same column of the table.*

Chain ID	% Accessibility (E. coli SecB)			
	Cys-76	Cys-97	Cys-102	Cys-113
A	0.49	0.09	0.91	0.80
B	0.00	5.64	1.14	4.25
C	0.00	11.86	0.00	16.04
D	0.00	14.59	0.25	5.57

Chain ID	% Accessibility/(*H. influenzae* SecB)			
	Cys-85	Cys-106	Cys-111	Leu-122
A	0.00	0.10	0.08	0.25
B	0.52	1.72	0.00	0.70
C	0.03	2.06	0.00	0.49
D	0.17	1.55	0.00	0.14

B. Shortest inter-cysteine Sγ distances for the cysteine residues that are the most probable sites of modification in modeled E. coli SecB.

Cysteine pair (Chain ID, Residue No.)	Inter-cysteine Sγ distance
	Å
A,97–C,97	24.77
A,97–C,102	25.58
A,102–C,97	24.12
A,102–C,102	23.96
B,97–D,97	24.08
B,97–D,102	23.06
B,102–D,97	23.77
B,102–D,102	21.58

ESR Studies of Site-specifically Spin-labeled BPTI Mutants—The ESR spectra of the different spin-labeled mutants of BPTI show the typical line-broadening that occurs upon covalent binding of the radicals to a protein. As a typical example, the spectra of the labeled mutant $(14–38)_{SL}$ are shown in Fig. 4. The fact that the line broadening is mainly observed as reduced signal amplitude of the high field signal (Fig. 4*A*) indicates that the bound radicals still have rather high mobility. This is consistent with the spin-labeled BPTI being in an unfolded state. Upon the addition of SecB, additional signals with a $2A_{zz}$ value of 63 G are apparent in the low and high field region of the ESR spectra (Fig. 4*B*, *1*, *1′*), indicating that binding of the labeled BPTI to the chaperone SecB has taken place. The relative area of peaks 1 and 1′ corresponds to ~50% of the total radicals, whereas the sharp signals of the highly mobile spin labels have decreased by about 50% as compared with Fig. 4*A* under normalized conditions. Such observations are indicative of restricted motional freedom of one of the two spin labels covalently bound to BPTI or by binding of ~50% of the labeled substrate protein. Similar spectra were observed by the authors in the case of lactate dehydrogenase (41), where the bound radical component was hardly visible at all but still accounted for 30% of the total spin-labeled substrate. The binding constant of unfolded BPTI for SecB under the conditions of the ESR experiments was determined to be 10 nM using fluorescence spectroscopy, an observation that is in agreement with findings described earlier (5, 39). Therefore, we assume that the sharp signals must originate from SecB-bound BPTI since there should be virtually no free BPTI present under the conditions used in the experiment (30 μM labeled BPTI in the presence of 300 μM SecB). Similar observations, *e.g.* decrease by 50% of the mobile component while an immobile spectral component representing about 50% of the total radical occurs, were made also for the binding of the BPTI mutants $(5–55)_{SL}$ and $(30–51)_{SL}$ (data not shown). The data suggest that SecB consistently interacts with only one of the two radicals within the mutant BPTI peptide chains.

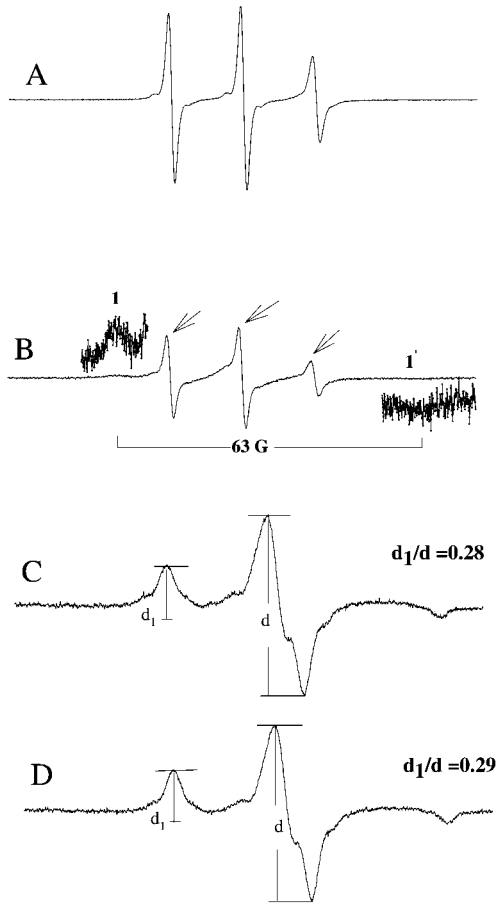

FIG. 4. **ESR spectra of spin labeled $(14–38)_{sl}$ mutant alone and in complex with SecB.** *A*, 30 μM of $(14–38)_{SL}$ alone at 298 K, pH 7.4. *B*, 30 μM of $(14–38)_{SL}$ in complex with 300 μM SecB at 298 K, pH 7.4. The *arrows* indicate the signal of the mobile fraction of the radical moiety that has decreased by about 50% upon binding to SecB. The absolute intensities in *A* and *B* are on an identical scale. *C*, ESR spectra of *A* recorded at 183 K; *D*, ESR spectra of *B* recorded at 183 K.

It was previously described that the extent of magnetic dipolar interaction between two spin-labeled cysteine side chains can be used to estimate the distance between bound radicals (22). To evaluate the line broadening due to static dipolar interactions, quantitative analysis of the inter-spin distance can be carried out in the absence of motion by acquiring the spectra in the frozen state (183 K). An estimation of the extent of broadening due to dipolar interaction is obtained from the line height ratio d_1/d (Fig. 4, *C* and *D*), which is in direct correlation to the average distance of the radicals from each other. In the absence of interaction (when a distance greater than 20 Å separates the radicals), a value of d_1/d of less than 0.4 is expected (22). Table II summarizes the d_1/d values of the three doubly labeled BPTI mutants in the presence and absence of SecB. The d_1/d ratio never reaches a value that would suggest dipolar interaction in the unbound state of BPTI. This indicates that the radicals bound to BPTI are further than 20 Å apart and that the conformation of the substrate bound to SecB is an extended one.

ESR Studies on the Chaperone SecB—SecB has four solvent-accessible cysteines (one per monomer), as assayed by the thiol reactive probes 5,5′-dithiobis(nitrobenzoic acid) and pyrene maleimide (33). The labeling, proteolysis, mass spectrometry, and modeling studies described above suggest cysteine 97 as the residue that is labeled. To obtain further insight into the possible conformational changes upon substrate binding, we have labeled the accessible cysteines using IOPI spin label. The

TABLE II
d_1/d values of spin-labeled mutants of BPTI alone (30 μM) and in complex with 300 μM SecB.

Mutant of BPTI	d_1/d −SecB	d_1/d +SecB
$(5–55)_{SL}$	0.32	0.26
$(30–51)_{SL}$	0.30	0.28
$(14–38)_{SL}$	0.28	0.29

ESR spectra of the spin-labeled chaperone indicate that the chaperone-bound radicals retain too much rotational freedom to determine the amount of dipolar spin-coupling from room temperature measurements (data not shown). Hence, low temperature spectra were acquired where the radicals were in a frozen state (Fig. 5*A*). The d_1/d value of the spectrum was determined to be 0.45, indicative of a relative, average distance of the radicals of about 20 Å or less (22). Line shape simulations using a program designed by Steinhoff *et al.* (42) resulted in a good fit of the spectrum in Fig. 5*A* (see *inset*) at an inter-spin distance of 14 ± 4.5 Å between the radicals. The addition of the unfolded substrate $(BPTI)_{all\ Ala}$ led to a drastic decrease in the d_1/d ratio to 0.36, whereas the $2A_{zz}$ value remained the same, indicating that the spin-labeled cysteines have moved apart from each other upon binding of the substrate protein (Fig. 5*B*). The spectra could be fitted well when the inter-spin distance of the radicals was set to 30 Å (where dipolar interactions cannot be observed) in the program (Fig. 5*B*, *inset*).

As described under "Materials and Methods," we used the model of the *E. coli* Sec B that we had obtained by aligning the *E. coli* sequence to the known crystal structure (36) and modeled a bound IOPI spin-label at position 97 of the *E. coli* sequence. The distance of between two NO radicals was determined to be ~18 Å, in excellent agreement with the value of 14 ± 4.5 Å determined from the line shape simulations described above. This is also consistent with the inter-cysteine distances indicated in Table IB and the length of the IOPI group, which spans about 7.5 Å from the nitroxide label to the site of attachment at the Sγ atom of Cys.

DISCUSSION

Both in prokaryotes and eukaryotes, proteins have to cross membranes either during or after their biosynthesis to reach their final destination. It is assumed that folded proteins are not translocation-competent. It has been suggested that during translocation proteins may be in a molten globule-like state (8). However the actual physical state of such proteins has not been well characterized. A variety of cellular chaperones that are involved in the protein translocation machinery of the cell have been found to play important roles in maintaining the nascent polypeptide chains in a non-native state. It is assumed that chaperones can bind to regions of the unfolded polypeptide chains, which are buried in the native state of the proteins (1). Thus, binding between chaperones and target substrate proteins is believed to be largely mediated by hydrophobic interactions, which is also a way of preventing nonspecific protein aggregation in the cell. The main function of the chaperone SecB is to maintain target precursor proteins in a translocation-competent state. We have investigated the free and the bound state conformations of both SecB and the model substrate protein, BPTI, by using either pyrene dyes or spin labels to study the spatial arrangement of different residues within both proteins. The studies were interpreted in light of the recently determined crystal structure of SecB from *H. influenzae*.

Proximity Relationships of Cysteines in Unfolded and SecB-bound BPTI—In aqueous solutions, pyrene probes that are covalently attached to a protein will equilibrate between stacked and unstacked configurations in the ground state if permitted by the local conformation of the protein. If flexible regions separate the pyrene moieties, the stacked configuration should dominate due to energetic reasons. Changes in the conformation of the protein near the pyrene probes will influence the equilibrium between stacked and unstacked pyrenes and will therefore change the ability to exhibit excimer fluorescence. Three different single-disulfide mutants of BPTI were used in the present work. Reduction of the disulfide bond results in two free cysteine thiol groups that can be chemically modified using SH-specific reagents such as maleimide or the iodo-oxopropylidene spin-label, IOPI. Reduction of the disulfide bond also results in denatured BPTI that functions as a substrate protein for SecB. The two BPTI mutants, with cysteines labeled at 5–55 and at 30–51 respectively, exhibit only weak excimer fluorescence (Fig. 1, *panels A* and *B*, *solid lines*). Strong excimer fluorescence is observed for a single disulfide mutant with pyrenes at positions 14–38, Fig. 1 (*panel C*, *solid line*). Excimer formation at the positions 14–38 may be enhanced by the presence of tertiary interactions within this region. These interactions are prevalent even in the unfolded state of the protein, as was indicated by two-dimensional ^1H NMR spectra of reduced BPTI and fluorescence energy transfer data on the collapsed molten coil state of BPTI (16, 19, 20). The data indicate that the two cysteine residues at positions 14 and 38 are in close proximity even in the unfolded state, whereas the cysteines at positions 5 and 55 as well as at 30 and 51 are farther apart from each other. The mutants of BPTI were also labeled with the cysteine-specific label IOPI and characterized by ESR. No effects due to dipolar interactions between radicals bound to the protein in close vicinity can be observed even in frozen solution (Fig. 4, *C* and *D* and Table II). The fact that excimer formation is visible for positions 14 and 38 but no dipolar interactions are observed in the corresponding ESR spectra may be explained by a rather small population of cysteines that are in close proximity. These may not be picked up in the ESR but are visible in the more sensitive fluorescence measurements. Alternatively, stacking of the aromatic pyrene residues may result in a small gain of energy that allows for a local folding minimum, which will not be formed when spin-labels are present instead. The addition of SecB to the unfolded, differently labeled BPTI mutants resulted in either a decrease or the total loss of excimer fluorescence, indicative of a conformational change within BPTI upon binding to the chaperone (Fig. 1, *A* through *C*, *dotted lines*). Excitation spectra were recorded to investigate whether ground state interactions occurred between the pyrenyl probes of the various labeled single disulfide mutants of BPTI. The excitation spectra were recorded from 280 to 360 nm for all the pyrene-labeled mutants in the presence and absence of SecB, and pyrene emission was monitored at 377 and 470 nm (25, 39). The two excitation spectra differ, and the peaks of the spectra detected at 470 nm are red-shifted, decreased in intensity, and broadened as compared with the peaks of the spectra detected at 377 nm, indicating that the pyrene moieties that show excimers had already formed dimers before excitation. In all the labeled BPTI mutants in the free and bound state, there is a red shift observed in the excitation spectra (data not shown). Also, the ratio of the fluorescence intensity ($F_{480\ nm}/F_{380\ nm}$) was found to vary with excitation wavelength, increasing slightly to the blue and sharply to the red of the minimum at 340 nm, in the free as well as the bound state (data not shown). This wavelength dependence of the fluorescence emission spectra as well as the broad red-shifted excitation spectra indicates a heterogeneous ground state environment for the pyrene chromophore in the labeled BPTI mutants even when bound to SecB. An increase in fluo-

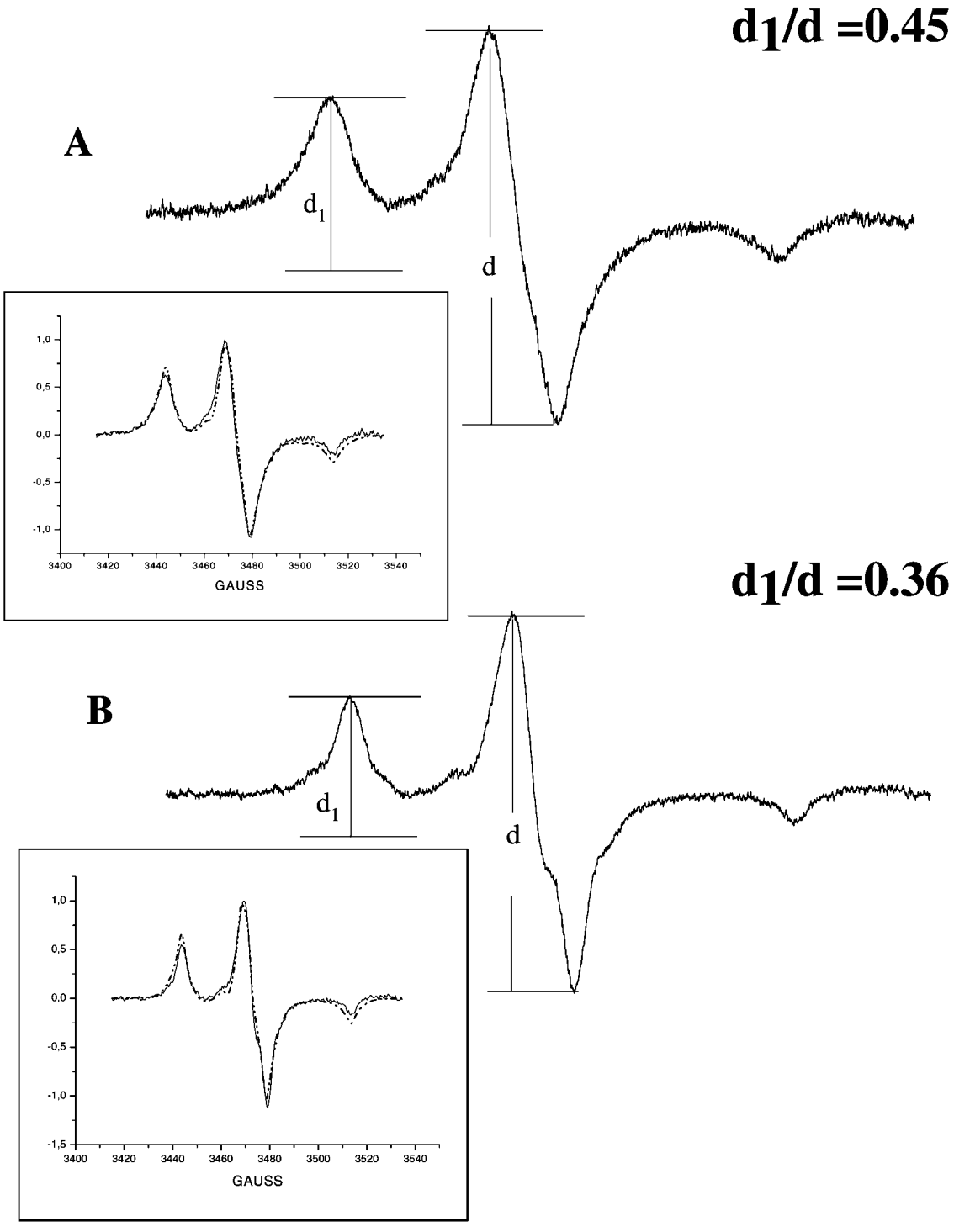

FIG. 5. **ESR spectra of spin labeled SecB in the presence and absence of $(BPTI)_{all\ Ala}$ at 183 K.** *A*, 20 μM of spin-labeled SecB alone; *B*, 20 μM of spin-labeled SecB in complex with 100 μM of $(BPTI)_{all\ Ala}$. The *insets* represent the computer-simulated ESR data using the program Dipfit (42).

rescence intensity was observed in all pyrene-labeled mutants upon binding to SecB, and all labeled mutants showed identical apparent binding affinities for SecB (K_d = 10 nM). All of the above is consistent with SecB binding to multiple regions on the target substrate rather than at a single site. Furthermore, the loss of excimer fluorescence upon binding to SecB is consistent with an extended conformation of the bound substrate protein.

Additional peaks in the high and low field area of the corresponding ESR spectra of the three different spin-labeled BPTI mutants clearly indicate that binding of the substrate proteins to SecB has taken place (Fig. 4). The relatively high $2A_{zz}$ value of 63 G is suggestive of a rather immobilized radical component that arises through binding of spin-labeled BPTI to a macromolecule like SecB. The fact that a second spectral component similar to the rather sharp signals of the unbound spin-labeled BPTI is present in the spectra and that the fraction of spins in the rigid environment are approximately equal to the mobile spins suggests that one of the spin labels on the modified BPTI is in direct contact with SecB, whereas the second one retains its mobility. This may be due to a rather extended form of the bound BPTI where the more mobile radical reaches further

away from the surface of the chaperone. The d_1/d values observed in the frozen state (Table II) of less than 0.4 are also consistent with an extended conformation of the bound substrate where no dipolar interactions can be observed. The ESR spectra both for the free and for the bound substrate are similar for all three mutants. Consistent with the fluorescence data, these observations indicate that SecB binds to multiple regions on the target substrate rather than at a single site. The smallest separation between the two labeled Cys residues is 21 residues in the 30–51 mutant. Since only one of the two residues is immobilized upon binding, the binding site on each SecB monomer of the tetramer must accommodate less than 21 residues. Isothermal titration calorimetric experiments used to study the interaction of unfolded BPTI with SecB also indicate that each SecB monomer can bind 10–30 residues in a solvent-exposed rigid cleft (9). Interestingly, when a sequence as short as 10 residues (of which three are basic) was inserted into alkaline phosphatase, this caused the translocation of alkaline phosphatase to become dependent on SecB *in vivo* (43). In addition, a recent study of SecB binding to peptide fragments from a number of proteins suggested that the binding site may be as short as nine residues (44) and that binding can occur at multiple sites on a substrate protein. A similar ESR study carried out using the B chain of insulin, a 26-residue peptide, also suggested that the binding frame of SecB is around 10 residues (39). This is entirely in agreement with results from the present study. In the recently determined crystal structure of SecB (36), a deep groove lined with aromatic amino acids (Subsite 1) was shown to have a length sufficient to accommodate a polypeptide stretch of 10 amino acids.

Conformational Transition of SecB upon Binding Substrate Protein—To investigate potential conformational changes within the structure of the chaperone SecB, we labeled the four solvent-accessible cysteine residues of the chaperone either with pyrene maleimide or with IOPI spin label. The presence of a single pyrene was confirmed by ESI-MS of the labeled protein. MALDI mass spectrometry analysis of the trypsin/CNBr cleavage of the pyrene-labeled SecB along with the depth and accessibility analysis showed that cysteine 97 is the most probable site of labeling.

No pyrene excimer formation was observed, suggesting that the corresponding modified cysteines are too far apart from each other to interact, in agreement with the modeled structure of SecB. However, upon addition of unfolded $(BPTI)_{all\ Ala}$, the fluorescence of the dye increases, indicating that a conformational change may have occurred.

ESR spectroscopy using SecB that was modified with an IOPI spin-label confirmed a conformational change within SecB upon binding of substrate (BPTI). ESR spectra of frozen solutions of the modified proteins where the radicals retain very low motional freedom exhibit a line-broadening of the signals that most likely results from dipolar interaction of at least two of the spin-labeled cysteines. The d_1/d ratio of 0.45 indicates a distance of the radicals of less than 20 Å (22). Line shape simulations as described in Steinhoff *et al.* (42) suggest that the distance between the radicals is 14 ± 4.5 Å. The data correlate very well with results from molecular modeling, where we calculated the inter-spin distances of IOPI spin-labels in the positions of cysteine 97 of the aligned structure for *E. coli* SecB. The structural model indicates a distance of 18 Å between the nitroxide radicals, which is within the 14 ± 4.5 Å distance determined by ESR, and computer simulation of the spectra.

Upon the addition of substrate protein, the d_1/d ratio decreased dramatically to 0.36, whereas the $2A_{zz}$ value remained identical, indicating that the radical moieties have moved apart from each other upon substrate binding. The distance between the radicals is then too large for dipolar interactions to occur. This is the first direct demonstration of a conformational change within SecB upon binding of a substrate protein.

Acknowledgments—We thank B. de Kruijff for kindly providing the SecB expression plasmid pJW25 and P. S. Kim and Mike Millholen for BPTI mutant plasmids. We thank M. K. Mathew for helpful discussions and G. Kraft, M. Kersten, and P. Guhr for help in recording spectra. We appreciate the help of H.-J. Steinhoff for providing the program Dipfit for simulating the ESR spectra.

REFERENCES

1. Hartl, F. U. (1996) *Nature* **381,** 571–580
2. Gething, M. & Sambrook, J. (1992) *Nature* **355,** 33–44
3. Weiss, J. B. & Bassford, P. J. (1990) *J. Bacteriol.* **172,** 3023–3029
4. Lecker, S. H., Driessen, J. M. & Wickner, W. (1990) *EMBO J.* **9,** 2309–2314
5. Fekkes, P., Blaauwen, T. & Driessen, A. J. M. (1995) *Biochemistry* **34,** 10078–10085
6. Panse, V. G., Udgaonkar, J. B. & Varadarajan, R. (1998) *Biochemistry* **37,** 14477–14483
7. Hardy, S. J. & Randall, L. L. (1991) *Science* **251,** 439–443
8. Bychkova, V., Krummeck, G. & Ptitsyn, O. B. (1988) *FEBS Lett.* **238,** 231–234
9. Panse, V. G., Swaminathan, C. P., Surolia, A. & Varadarajan, R. (2000) *Biochemistry* **39,** 2420–2427
10. Staley, J. P. & Kim, P. S. (1994) *Protein Sci.* **3,** 1822–1832
11. Darby, N. J., Morin, P. E., Talbo, G. & Creighton, T. E. (1995) *J. Mol. Biol.* **249,** 463–477
12. Dadlez, M. & Kim, P. S. (1996) *Biochemistry* **35,** 16153–16164
13. Schulman, B. A., & Kim, P. S. (1994) *Protein Sci.* **3,** 2226–2232
14. Amir, D. & Haas, E. (1988) *Biochemistry* **27,** 8889–8893
15. Amir, D., Krausz, S. & Haas, E. (1992) *Proteins* **13,** 162–173
16. Gottfried, D. S. & Haas, E. (1992) *Biochemistry* **31,** 12353–12362
17. Gussakovsky, E. E. & Haas, E. (1992) *FEBS Lett.* **308,** 146–148
18. Pan, H., Barbar, E., Barnay, G. & Woodward, C. (1995) *Biochemistry* **34,** 13974–13981
19. Ferrer, M., Barany, G. & Woodward C. (1995) *Nat. Struct. Biol.* **2,** 211–217
20. Lumb, K. J. & Kim, P. S. (1994) *J. Mol. Biol.* **236,** 412–420
21. Hubbell, W. L., Gross, A., Langen, R. & Lietzow, M. A. (1998) *Curr. Opin. Struct. Biol.* **8,** 649–656
22. Rabenstein, M. D. & Shin, Y. K. (1995) *Proc. Natl. Acad. Sci. U. S. A.* **92,** 8239–8243
23. Farrens, D. L., Altenbach, C., Yang, K., Hubbell, W. L. & Khorana, H. G. (1996) *Science* **274,** 768–770
24. Altenbach, C., Yang, K., Farrens, D. L., Farahbakhsh, Z. T., Khorana, H. G., & Hubbell, W. L. (1996) *Biochemistry* **35,** 12470–12478
25. Lehrer, S. S. (1997) *Methods Enzymol.* **278,** 286–295
26. Zhao, M., Zen, K. C., Hubbell, W. L. & Kaback, H. R. (1999) *Biochemistry* **38,** 7407–7412
27. Sun, J., Voss, J., Hubbell, W. L. & Kaback, H. R. (1999) *Biochemistry* **38,** 3100–3115
28. Laemmli, U. K. (1970) *Nature* **277,** 680–685
29. Fasman, G. D., Park, K. & Randall, L. (1995) *J. Protein Chem.* **14,** 595–600
30. Staley, J. P., & Kim, P. S. (1992) *Proc. Natl. Acad. Sci. U. S. A.* **89,** 1519–1523
31. Volodarsky L. B. (1988) in *Imidazoline Nitroxides*, Vol. 1, CRC Press, Inc., Boca Raton, FL
32. Creighton, T. E. (1990) *Protein Structure: A Practical Approach*, pp. 155–166, IRL Press at Oxford University Press, Oxford
33. Panse, V. G., Swaminathan, C. P., Aloor, J. J., Surolia, A. & Varadarajan, R. (2000) *Biochemistry* **39,** 2362–2369
34. Darbre, A. (ed) (1986) in *Practical Protein Chemistry: A Handbook*, Wiley Interscience, Chichester, Great Britain
35. Sali, A. & Blundell, T. L. (1993) *J. Mol. Biol.* **234,** 779–815
36. Xu, Z., Knafles J. D. & Yoshino K. (2000) *Nat. Struct. Biol.* **7,** 1172–1177
37. Chakravarty S. & Varadarajan, R. (1999) *Structure* (*Lond.*) **7,** 723–732
38. Lee, B. & Richards, F. M. (1971) *J. Mol. Biol.* **55,** 379–400
39. Panse, V. G., Vogel, P., Trommer, W. E. & Varadarajan, R. (2000) *J. Biol. Chem.* **275,** 18698–18703
40. Topping, T. B., Woodbury, R. L., Diamond, D. L., Hardy, S. J. & Randall, L. L. (2001) *J. Biol. Chem.* **276,** 7437–7441
41. Wenzel, H. R., Pfleiderer, G., Trommer, W. E., Paschenda, K., and Redhardt, A. (1976) *Biochim. Biophys. Acta* **452,** 292–301
42. Steinhoff, H.-J, Radzwill, N., Thevis, W., Lenz, V., Brandenburg, D., Antson, A., Dodson, G. & Wollmer, A. (1997) *Biophys. J.* **73,** 3287–3298
43. Kim, J. & Kendall, D. A. (1998) *J. Bacteriol.* **180,** 1396–1401
44. Knoblauch, N. T., Rudiger, S., Schonfeld, H. J., Driessen, A. J., Schneider-Mergener, J. & Bukau, B. (1999) *J. Biol. Chem.* **274,** 34219–34225